

SPATIALLY-VARIANT LUCY-RICHARDSON DECONVOLUTION FOR MULTIVIEW FUSION OF MICROSCOPICAL 3D IMAGES

Maja Temerinac-Ott^{1,2}, Olaf Ronneberger^{1,2}, Roland Nitschke^{2,3}, Wolfgang Driever^{2,4} and Hans Burkhardt^{1,2}

¹Institute of Computer Science, Albert-Ludwigs-University of Freiburg,
Chair of Pattern Recognition and Image Processing, Georges-Köhler-Allee Geb. 052,
79110 Freiburg, Germany, temerina@informatik.uni-freiburg.de

² BIOS Centre for Biological Signalling Studies, Albert-Ludwigs-University of Freiburg, Germany

³ ZBSA, Live Imaging Center, Albert-Ludwigs-University Freiburg, Germany

⁴ Faculty of Biology, Albert-Ludwigs-University Freiburg, Germany

ABSTRACT

A framework for fast multiview fusion of Single Plane Illumination Microscopy (SPIM) images based on a spatially-variant point spread function (PSF) model is presented. For the multiview fusion a new algorithm based on the regularized Lucy-Richardson deconvolution and the Overlap-Save method is developed and tested on SPIM images. In the algorithm the image is decomposed into small blocks which are processed separately thus saving memory space and allowing for parallel processing.

Index Terms— Lucy-Richardson deconvolution, spatially-variant PSF, total variation, SPIM

1. INTRODUCTION

SPIM [1] is a powerful tool for recording deep inside live embryos. It combines the advantages of widefield and confocal microscopy to produce images of high resolution of e.g. zebrafish embryos. One of the advantages of SPIM is its mounting technique inside a gel cylinder which makes the objects to be recorded easily movable. Thus one is able to rotate the gel cylinder and take images from the same object from different views (Fig. 1). In this way absorption and scattering are compensated by taking another image of the same sample from a slightly different angle. The resulting recordings comprise a number of different views of the same object which need to be 1. registered and 2. fused.

SPIM is as fast as widefield microscopy since it records the whole image plane at once, however, it only illuminates one plane at a time using a light sheet which keeps the scattering small. To create a uniform light sheet across the whole field of view is difficult. The PSF of the system will vary from the middle to the border of the light sheet making modeling of a spatially-variant PSF necessary.

This study was supported by the Excellence Initiative of the German Federal Governments (EXC 294) and the SFB 592.

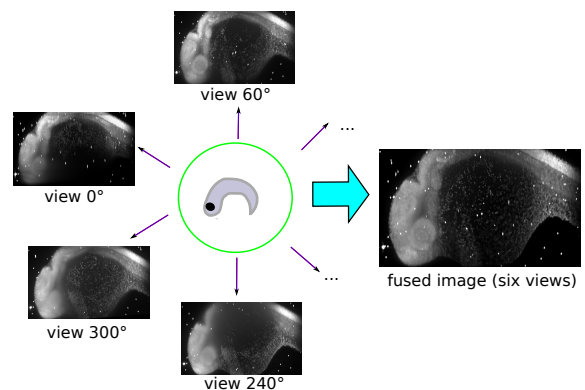


Fig. 1. Six images recorded from different views with SPIM are fused to one image using the proposed method.

In this work we propose a new framework for the SPIM reconstruction. Our goal is to keep memory space and computation time as low as possible in order to make the technology feasible for everyday use in the lab. After registration, the images are decomposed into small blocks, that can be processed independently from each other. The multiview-fusion is conducted using Overlap-Save (OS) deconvolution and the regularized Lucy-Richardson (LR) algorithm. This results in three advantages over already existing methods: 1. A spatially-variant PSF can be modeled, 2. Only small amounts of memory is used and 3. the algorithm can be performed using parallel computation.

2. RELATED METHODS

Many solutions for improving the reconstruction of SPIM images have already been proposed (e.g. [2], [3], [4]). In [2] the registration of the views was performed using a precise calibration of the microscope. This approach has two ma-

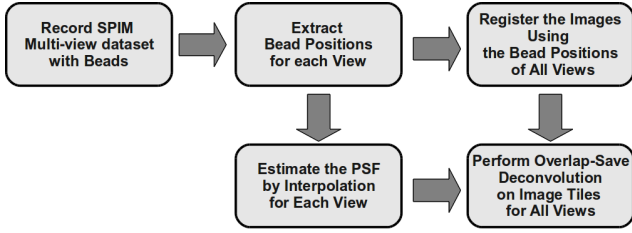


Fig. 2. The general framework for the block-based multiview fusion.

major drawbacks: 1. after calibration the microscope should not move at all and 2. the verification of the registration results on a pixel basis is very difficult. These two drawbacks were overcome in [3] by inserting fluorescent point markers (beads) into the surrounding medium of the object. Thus the precision of the registration can be exactly expressed as the distance between corresponding beads. The computation of the transformation is then no longer affected by the calibration of the system and the computation time and memory requirements are very low, since only point set coordinates are compared.

For the fusion there are two common solutions: 1. to combine the gray values directly or 2. multi-view deconvolution of several stacks. The first solution uses simple operators such as maximum, average or more elaborate methods such as weighted blending [3]. The first kind of methods require low computation time, however they do not account for deformations introduced by the PSF. The second kind of methods which are based on deconvolution are much slower. They depend on the correct estimation of the PSF and can produce undesired artifacts. Also, they are more time consuming and if performed on the whole image require more memory. So far in [2], [5] one (spatially-invariant) PSF was assumed per view.

3. OVERVIEW OF THE FRAMEWORK

Our general framework is presented in Fig. 2. First a biological sample is recorded from different angles using SPIM. Second the bead positions are extracted with morphological operators. Third the beads are used for the registration of the different views. Fourth the point spread function of the beads is estimated at the bead positions. Finally, using OS method and the multiview LR algorithm the image is deconvolved and fused at the same time.

For the extraction of the beads the image is smoothed by a Gaussian filter and local maxima are computed, which are the candidates for the bead positions. The image is then binarized by computing a threshold with Otsu’s method [6]. Next the specimen is roughly segmented by computing the largest connected component in the binarized image. Local maxima

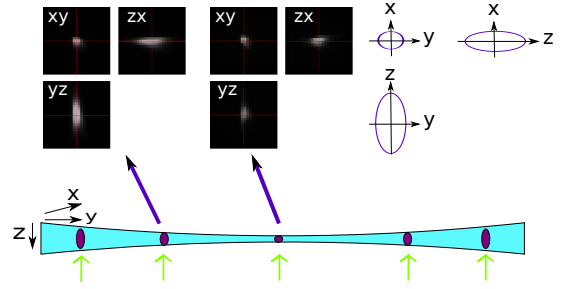


Fig. 3. The PSF size changes along the lightsheet in y -direction. The beads in the middle of the lightsheet (upper center image) are small and at the border of the lightsheet (upper left image) are large.

lying outside the specimen are saved as bead coordinates.

For the registration of the images local descriptors based on Group Averaging [7] are extracted in order to find corresponding beads between two views. The found correspondences are used to compute the pairwise affine transform. Then a groupwise optimization of the transform parameters is performed iteratively until no new correspondences are found.

A PSF estimate is obtained by extracting a window of size r around each bead coordinate. If two bead coordinates are too close, the PSF estimate will be discarded. In Fig. 3 two differing beads from the same image stack are presented; the PSF of the beads is elongated when the light sheet gets thicker towards the border of the image stack.

For image fusion, the Lucy-Richardson Multiview Overlap-Save Method Using Total Variation (denoted as “LRMOS-TV”) has been developed.

4. LUCY-RICHARDSON MULTIVIEW OVERLAP-SAVE METHOD USING TOTAL VARIATION (“LRMOS-TV”)

The main novelty of the proposed LRMOS-TV algorithm is to combine regularized multiview LR and OS deconvolution. The combined methods enable to model the spatially variant PSF function estimated by the beads.

4.1. Lucy-Richardson Deconvolution

In [8], [9] Lucy and Richardson develop an iterative expectation maximization deconvolution algorithm based on a Bayesian framework. Since SPIM image statistics can be modeled by a Poisson process, the likelihood probability is formulated as ([10]):

$$p(Y|X) = \prod_{\mathbf{v}} \frac{[(H * X)(\mathbf{v})]^{Y(\mathbf{v})} \cdot e^{-(H * X)(\mathbf{v})}}{Y(\mathbf{v})!}, \quad (1)$$

where $X, Y, H : \mathbb{R}^3 \rightarrow \mathbb{R}, \mathbf{v} \in \mathbb{R}^3$. Hereby X denotes the true image, Y the recorded image and H the PSF of the system. The likelihood probability Eq. (1) is maximized by minimizing the negative log likelihood. Thus it is enough to minimize the functional $J(X)$ defined as:

$$J(X) = \int_{\mathbf{v}} (H * X)(\mathbf{v}) - Y(\mathbf{v}) \log[(H * X)(\mathbf{v})] d\mathbf{v}. \quad (2)$$

As a result the following iteration procedure is derived:

$$\hat{X}^{p+1}(\mathbf{v}) = \hat{X}^p(\mathbf{v}) \cdot C^p(\mathbf{v}), \quad (3)$$

where \hat{X}^p is the current estimate of the original image X at iteration p and C^p is the correction factor defined as:

$$C^p(\mathbf{v}) = \left(H' * \frac{Y}{S^p} \right) (\mathbf{v}), \quad (4)$$

where $S^p = H * \hat{X}^p$ is the simulated recorded image and $H'(\mathbf{v}) = H(-\mathbf{v})$.

4.2. Regularization of the Lucy-Richardson Algorithm

For noisy images, the LR algorithm amplifies the noise and thus regularization is required to obtain a smooth solution. In [11] Total Variation (TV) is used for regularization of the LR algorithm. TV preserves the borders and suppresses the noise. The deconvolution algorithm presented in the previous section is regularized by adding the TV term to the functional J , resulting in the functional J_{TV} :

$$J_{TV}(X) = J(X) + \lambda \int_{\mathbf{v}} |\nabla X(\mathbf{v})| d\mathbf{v}, \quad (5)$$

where $|\cdot|$ denotes the L2-norm. In the LR algorithm this results in dividing the image \hat{X}^p in Eq. (3) by a factor:

$$\hat{X}^{p+1}(\mathbf{v}) = \frac{\hat{X}^p(\mathbf{v})}{1 - \lambda \operatorname{div} \left(\frac{\nabla \hat{X}^p(\mathbf{v})}{|\nabla \hat{X}^p(\mathbf{v})|} \right)} \cdot C^p(\mathbf{v}) \quad (6)$$

4.3. Multiview Lucy-Richardson Algorithm

In [5] the original LR algorithm is extended for multiview fusion. For N recordings (Y_1, \dots, Y_N) and the corresponding PSFs (H_1, \dots, H_N), the new correction factor C is computed as an average of the individual correction factors C_i :

$$C^p = \frac{1}{N} \sum_{i=1}^N C_i^p \quad (7)$$

$$C_i^p(\mathbf{v}) = \left(H'_i * \frac{Y_i}{S_i^p} \right) (\mathbf{v}) \quad (8)$$

$$S_i^p(\mathbf{v}) = \left(H_i * \hat{X}^p \right) (\mathbf{v}). \quad (9)$$

Algorithm 1. LRMOS-TV

```

for  $m = 1$  to  $T_1$  do
  for  $n = 1$  to  $T_2$  do
    for  $k = 1$  to  $T_3$  do
      1. Extract extended region  $R_i = Y_{mnk}^{(r+s)}$ 
      from  $Y_i$  for each view  $i$ .
      2. Obtain  $H_i = H_{m,n,k}^{(r+s)}$ 
      by padding with zeros for each view  $i$ .
      3. Compute the initial estimate:
       $\hat{X}^0 = \frac{1}{N} \sum_{i=1}^N R_i^p$ 
      4. Iterate:
       $\hat{X}_{m,n,k}^{p+1}(\mathbf{v}) = \frac{\hat{X}_{m,n,k}^p(\mathbf{v})}{1 - \lambda \operatorname{div} \left( \frac{\nabla \hat{X}_{m,n,k}^p(\mathbf{v})}{|\nabla \hat{X}_{m,n,k}^p(\mathbf{v})|} \right)} \cdot C^p(\mathbf{v})$ 
      5. Extract  $\hat{X}_{mnk}$  from  $\hat{X}_{mnk}^{(r+s)}$  and save into  $\hat{X}$ .
    end for
  end for
end for

```

4.4. Overlap-Save Deconvolution

This approach is based on the assumption that the blur is approximately spatially invariant in small regions of the image domain. The image is partitioned into blocks, restoring each local region using its corresponding spatially invariant PSF. The results are then put together to obtain the restored image. Blocking artifacts are reduced by taking larger overlapping regions from the recorded image for restoration and then extracting only the inner part after restoration ([12]).

4.5. Proposed Algorithm

The convolved image is partitioned in blocks of size s ; the size of the PSF function H_{mnk} is r . For fast processing s and r are selected such that $s + r = 2^l$. For 3D images of size ($N_1 \times N_2 \times N_3$) the partitioning results in $T_1 \cdot T_2 \cdot T_3$ blocks, where $T_i = \lfloor N_i/s \rfloor$. $Y_{mnk}^{(r+s)}$ denotes the block Y_{mnk} of size $s \times s \times s$ padded by pixels in its neighborhood of size r .

For the computation of each block $\hat{X}_{m,n,k}$, extended regions R_i and PSF functions H_i are extracted from each view. The PSF at position n, m, k is linearly interpolated from n PSFs in its neighborhood:

$$H_i(\mathbf{v}) = \frac{1}{\sum_{n=1}^P w_n} \sum_{n=1}^P w_n H_{i,n}(\mathbf{v}).$$

The weights w_n are computed proportional to the inverse Euclidean distance of the available PSF coordinate to the desired PSF position. We consider $P = 4$, meaning the four nearest available PSFs are interpolated. The regularized multiview LR deconvolution is performed for K iterations. Only the inner part of the deconvolved block is then saved into the final image \hat{X} .

5. RESULTS ON SPIM IMAGES

24h old zebrafish images recorded from six views using SPIM are fused using the proposed framework. The zebrafish is stained with Sytox and embedded in a Glycerol solution filled with latex-fluorophore beads of $1\mu m$ diameter. A W-Plan - Apochromat (20x/1.0 M27) lens is used and each view is illuminated from two sides resulting in two images per view. The two images are fused by averaging to produce a more evenly illuminated image. The sample is rotated in 60° steps around the y -axis. The resulting images have a size of $(751 \times 1040 \times 1388)$ with voxels of size $(1\mu m \times 1.10897\mu m \times 1.10897\mu m)$.

In the LRMOS-TV algorithm five iterations are performed per block, where $\lambda = 0.0001$, $r = 11$ and blocks of size 64 are used. When computed with Matlab (R2009a) on a 4x QuadCore Xeon X7350 2.93GHz CPU the computation time is 45 minutes for the fusion of the six views scaled to the voxel size of $2\mu m$.

5.1. Comparison to State-Of-the-Art Software

The Fiji-plugin [3] with multiband blending was used for the fusion of the six views as well. LRMOS-TV fusion can better reconstruct the cell borders and textures than blending, since we apply a better model to the optical properties of the system (Fig. 6).

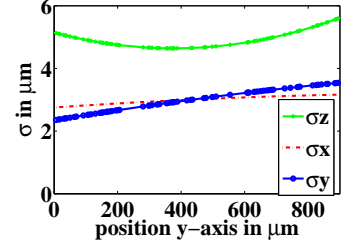
In Fig.7 MIPs for the yz - and the xz - view before (Fig.7(a)) and after reconstruction by blending (Fig.7(b)) and the LRMOS-TV algorithm (Fig.7(c)) are presented. After reconstruction the absorbed and occluded parts of the image are visible. As expected the beads at the image borders are rather round after applying the LRMOS-TV algorithm (Fig.7(c)). After blending the beads at the border are more star shaped (Fig.7(b)) which is an undesired effect.

5.2. Quantitative Evaluation

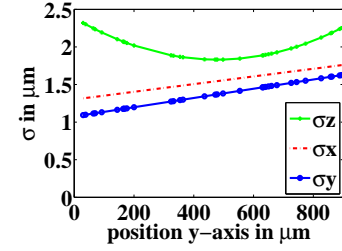
Since the beads are randomly placed in the whole image, we do not have an estimate of the PSF at every image position. Thus we need to interpolate the PSF at positions where no bead has been placed. In order to check for robustness of our method at positions where no bead is present, we divide the image in two parts (upper and lower) along the x -axis. Herby we assume that the PSF along the x -direction of the lightsheet does not change. Thus the PSFs estimated in the lower part of the x -axis are a good estimate for the PSFs in the upper part. Next the PSFs from the lower part are used to deconvolve the upper part, thus using the beads in the upper part as phantoms in order to measure the quality of the deconvolution.

The quality is measured using the standard deviation of the beads $\sigma_x, \sigma_y, \sigma_z$ computed as (e.g. for the x -axis):

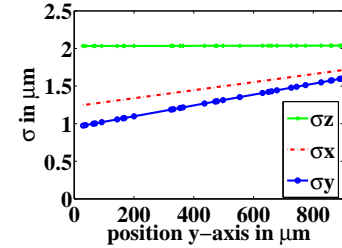
$$\sigma_x = \sqrt{\int_{\mathbf{v} \in \mathbb{R}^3, \|\mathbf{v} - \mathbf{v}_0\|_2 < r} (x - x_0)^2 \hat{X}(\mathbf{v}) d\mathbf{v}}.$$



(a) original bead shape (single image)



(b) deconvolved with average PSF (fused image, upper half)



(c) deconvolved with variant PSF (fused image, upper half)

Fig. 4. The standard deviation σ along x, y, z -axis of a Gaussian fitted to the beads depending on their position in the y -plane for (a) the original image, (b) the six images deconvolved by the average PSF and (c) by LRMOS-TV.

Herby $\mathbf{v} = (x, y, z)$ denotes the position in the image \hat{X} and $\mathbf{v}_0 = (x_0, y_0, z_0)$ is the center of the detected bead.

Fig.4(a) shows that σ_x and σ_y in the original image do not vary much along the y -plane, whereas σ_z is large at the border and smaller in the middle of the image. After multiview deconvolution ([5]) of the six views with the average PSF (Fig.4(b)) σ_z is reduced however the variation of σ_z along the y -plane remains. After applying LRMOS-TV (Fig.4(c)) σ_z is nearly constant along the y -plane, thus reflecting the real shape of the spherical beads.

The overall mean of the standard deviations measured in the upper part of the images deconvolved with the lower part average PSF and the spatially-variant PSFs is given in Tab. 1. Here the average PSF model is slightly better in the mean of the σ_z , however worse for the mean σ_x and the mean σ_y . This

	deconvolved with average PSF	deconvolved with variant PSF
σ_x	1.5375 (max 1.6409)	1.4835 (max 1.6179)
σ_y	1.3598 (max 1.7707)	1.2937 (max 1.7233)
σ_z	2.0252 (max 2.4188)	2.0354 (max 2.038)

Table 1. The mean (and max) standard deviation of the beads in the upper part of the image after deconvolution with the PSFs estimated from the lower part of the image.

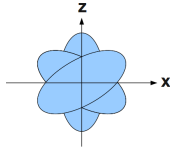


Fig. 5. The bead shape in zx -direction overlaid for six views.

is due to the noise estimated in the lower part of the image and then applied to the upper part when using the spatially-variant PSF model. The noise in the middle is reduced by using the average PSF model.

Ideally, $\sigma_x \approx \sigma_y \approx \sigma_z$, if perfectly round beads are considered. The higher value of σ_z can be explained by the choice of the recorded angles. Fig. 5 shows the real space covered by the six views. In order to compensate the extension in the z -axis, an orthogonal recording of the same bead is required. For an isotropic reconstruction of the beads, eight views with angle 45° should be preferred over six views with angle 60° .

6. CONCLUSIONS

A new framework for the fusion of SPIM images was presented based on the Overlap-Save regularized Lucy-Richardson deconvolution. Using LRMOS-TV the beads in the whole image can be better reconstructed than by using only one PSF for the whole image. For further processing e.g. segmentation the LRMOS-TV deconvolution can be very helpful since it enhances the structure's border.

Further topics of research will include additional regularization strategies (e.g. Wavelet based regularization) as well as the optimal number of iteration steps. A parametric model of the PSF along the lightsheet should be developed in order to reduce the noise and decrease the influence from the image sampling grid. For better precision, beads will be inserted in the animal in order to model the PSF inside the object. Further improvement could be achieved by choosing the block sizes depending on the variation of the PSF instead of choosing constant block size.

7. REFERENCES

- [1] J. Huisken, J. Swoger, F. Del Bene, J. Wittbrodt, and E. H. K. Stelzer, "Optical sectioning deep inside live embryos by selective plane illumination microscopy," *SCIENCE*, vol. 305, pp. 1007–1009, August 2004.
- [2] J. Swoger, P. Verveer, K Greger, J. Huisken, and E. H. K. Stelzer, "Multi-view image fusion improves resolution in three-dimensional microscopy," *Opt. Express*, vol. 15, no. 13, pp. 8029–8042, 2007.
- [3] S. Preibisch, S. Saalfeld, J. Schindelin, and P. Tomancak, "Software for bead-based registration of selective plane illumination microscopy data," *Nature Methods*, vol. 7, pp. 418–419, 2010.
- [4] P. J. Keller, A. D. Schmidt, A. Santella, K. Khairy, Z. Bao, J. Wittbrodt, and E. H. K. Stelzer, "Fast, high-contrast imaging of animal development with scanned light sheetbased structured-illumination microscopy," *Nature Methods*, vol. 7, pp. 637–42, 2010.
- [5] U. Krzic, *Multiple-view microscopy with light-sheet based fluorescence microscope*, Ph.D. thesis, Rupert-Carola University of Heidelberg, 2009.
- [6] N. Otsu, "A threshold selection method from gray-level histograms," *Systems, Man and Cybernetics, IEEE Transactions on*, vol. 9, no. 1, pp. 62–66, jan. 1979.
- [7] M. Temerinac-Ott, M. Keuper, and H. Burkhardt, "Evaluation of a new point clouds registration method based on group averaging features," in *Proc. of ICPR 2010*, 2010, pp. 2452–2455.
- [8] L. B. Lucy, "An iterative technique for the rectification of observed distributions," *The Astronomical Journal*, vol. 79, no. 6, pp. 745–754, 1974.
- [9] W. H. Richardson, "Bayesian-based iterative method of image restoration," *Journal of the Optical Society of America*, vol. 62, no. 1, pp. 55–59, 1972.
- [10] T. Hebert and R. Leahy, "A generalized em algorithm for 3-d bayesian reconstruction from poisson data using gibbs priors," *Medical Imaging, IEEE Transactions on*, vol. 8, no. 2, pp. 194–202, jun 1989.
- [11] N. Dey, L. Blanc-Feraud, C. Zimmer, Z. Kam, J.-C. Olivo-Marin, and J. Zerubia, "A deconvolution method for confocal microscopy with total variation regularization," in *Proc. of ISBI 2004*, 2004, pp. 1223–1226.
- [12] J. G. Nagy and D. P. O'Leary, "Fast iterative image restoration with a spatially varying psf," in *Advanced Signal Processing: Algorithms, Architectures, and Implementations VII*, Franklin T. Luk, Ed. 1997, vol. 3162, pp. 388–399, SPIE.

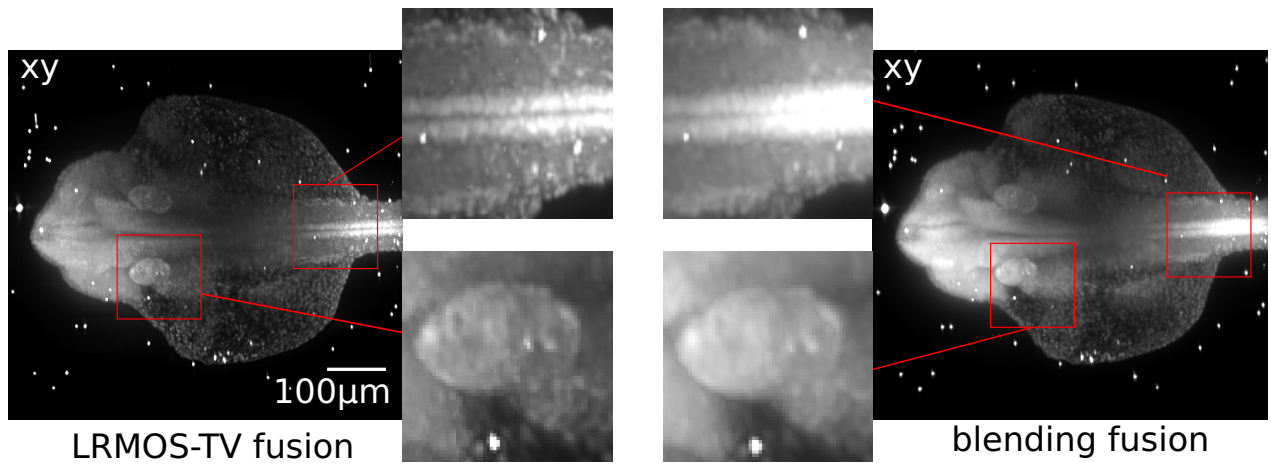


Fig. 6. Comparison of the Maximum Intensity Projections (MIP) after applying the proposed LRMOS-TV fusion (left) and the blending fusion [3] (right).

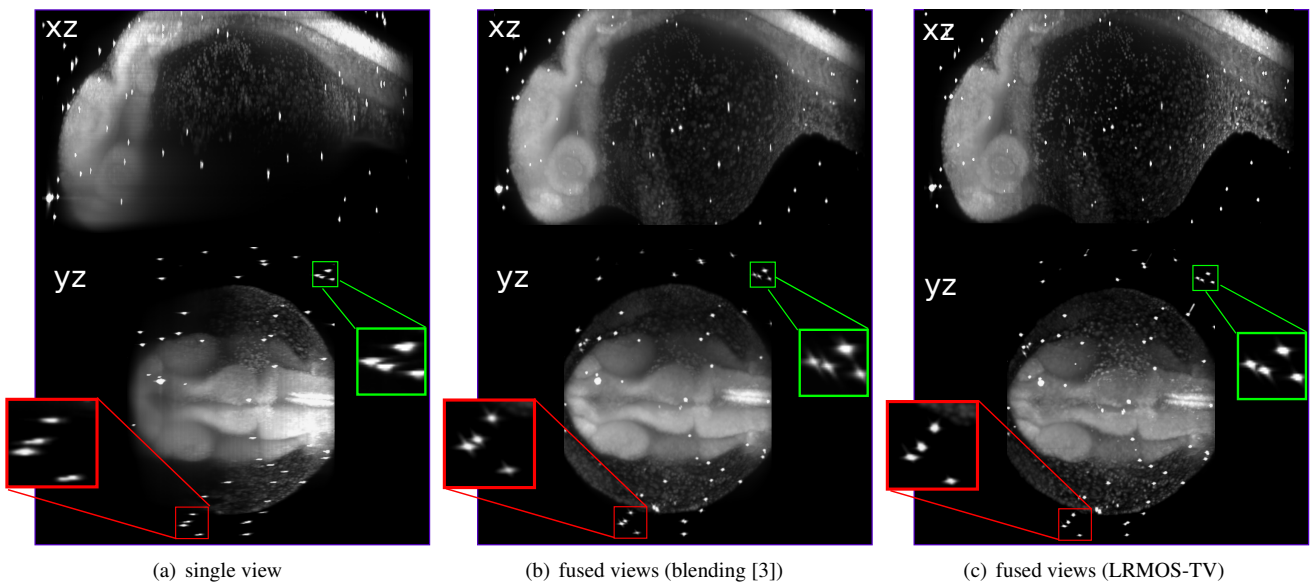


Fig. 7. The MIPs of the original angle 0 (a) and the reconstruction of the missing information from the five remaining views in (b) by blending and in (c) by the proposed method.